Epigenetic Flexibility Underlies Somaclonal Sex Conversions in Hexaploid Persimmon

Kanae Masuda[1], Takashi Akagi [1,2,*], Tomoya Esumi[3] and Ryutaro Tao[4]

[1]Graduate School of Environmental and Life Science, Okayama University, Okayama, 700-8530 Japan
[2]Japan Science and Technology Agency, PRESTO, Kawaguchi-shi, Saitama, 332-0012 Japan
[3]Academic Assembly Institute of Agricultural and Life Sciences, Shimane University, Matsue, 690-8504, Japan
[4]Graduate School of Agriculture, Kyoto University, Kyoto, 606-8502 Japan
*Corresponding author: E-mail, takashia@okayama-u.ac.jp; Fax, +81-75-753-6497.

Epigenetic regulation adds a flexible layer to genetic variations, potentially enabling long-term, but reversible, changes to a trait, while maintaining genetic information. In the hexaploid Oriental persimmon (*Diospyros kaki*), genetically monoecious cultivars bearing male flowers require the Y-encoded small RNA (smRNA) gene, *OGI*. This gene represses the expression of its autosomal counterpart gene, *MeGI*, as part of the canonical male production system. However, a *D. kaki* cultivar, Saijo, which lacks the *OGI* gene and originally bears only female flowers, occasionally produces somaclonal mutant male and revertant female (RF) branches. In this study, we investigated the mechanisms underlying these somaclonal sex conversions in persimmon. Specifically, we aimed to unravel how a genetically female tree without the *OGI* gene can produce male flowers and RF flowers. Applying multi-omics approaches, we revealed that this noncanonical male production system is basically consistent with the canonical system, in which the accumulation of smRNA targeting *MeGI* and the considerable DNA methylation of *MeGI* are involved. The epigenetic status of *MeGI* on CGN and CHG was synchronized to the genome-wide methylation patterns, both in transition to and from the male production system. These results suggest that the somaclonal sex conversions in persimmon are driven by the genome-wide epigenetic regulatory activities. Moreover, flexibility in the epigenetic layers of long-lived plant species (e.g. trees) is important for overcoming genetic robustness.

Keywords: DNA methylation ● Epigenetic variation ● Multi-omics ● Sex determination ● Somaclonal mutation.

Accession numbers: The nucleotide sequence included in this paper has been submitted to DDBJ.

Introduction

Sexual reproduction is the main biological process that maintains genetic diversity within a species. Nevertheless, among plants, most angiosperms are hermaphroditic, which is thought to be the ancestral state of the sexual system in flowering plants (Ainsworth 2000). In addition, some plant species have evolved distinct sexual systems, including monoecy (i.e. formation of male and female flowers by one plant) or dioecy (i.e. separate male and female plants; Renner 2014). The formation of unisexual flowers in a monoecious system depends on internal factors, such as plant hormone balances (Martin et al. 2009, Hartwig et al. 2011), whereas the unisexuality of individuals in a dioecious system is often associated with genetic determinants on the sex chromosomes (Ming et al. 2011, Henry et al. 2018). Regarding dioecy, only a few genetic determinants have been identified in some lineages, including persimmon (*Diospyros* spp.; Akagi et al. 2014a), garden asparagus (*Asparagus officinalis* L.; Harkess et al. 2017, Murase et al. 2017, Tsugama et al. 2017) and kiwifruit (*Actinidia* spp.; Akagi et al. 2018, Akagi et al. 2019a). In dioecious persimmon species, a Y chromosome-encoded small RNA (smRNA) gene, *OGI*, which is believed to be the only sex determinant, is responsible for repressing the expression of the autosomal counterpart, *MeGI* (Akagi et al. 2014a, Henry et al. 2018, Yang et al. 2019). A recent polyploidization event in wild diploid species that generated the cultivated hexaploid Oriental persimmon (*Diospyros kaki*) established a plastic sex-determination system in which genetically male plants carrying at least one copy of the Y chromosome-encoded *OGI* gene exhibit monoecy, whereas individuals carrying only X chromosomes are females (Akagi et al. 2016a, Akagi et al. 2016b). The basic physiological mechanism mediating the formation of male flowers in hexaploid monoecious *D. kaki* individuals is likely identical to that in diploid dioecious male individuals and depends on the repression of *MeGI* expression. However, in *D. kaki*, *OGI* expression is substantially inactivated because of the presence of an SINE-like transposon in the promoter region. Moreover, the epigenetic conditions in the *MeGI* promoter region can influence flower sex determination in monoecious trees (Akagi et al. 2016a, Henry et al. 2018). The epigenetic conditions in the *MeGI* promoter region are highly associated with the accumulation of smRNA targeting *MeGI*, thereby repressing *MeGI* expression (Akagi et al. 2016a; **Fig. 1A**).

In addition to Oriental persimmon, epigenetic conditions are often associated with the sex determination of other plant
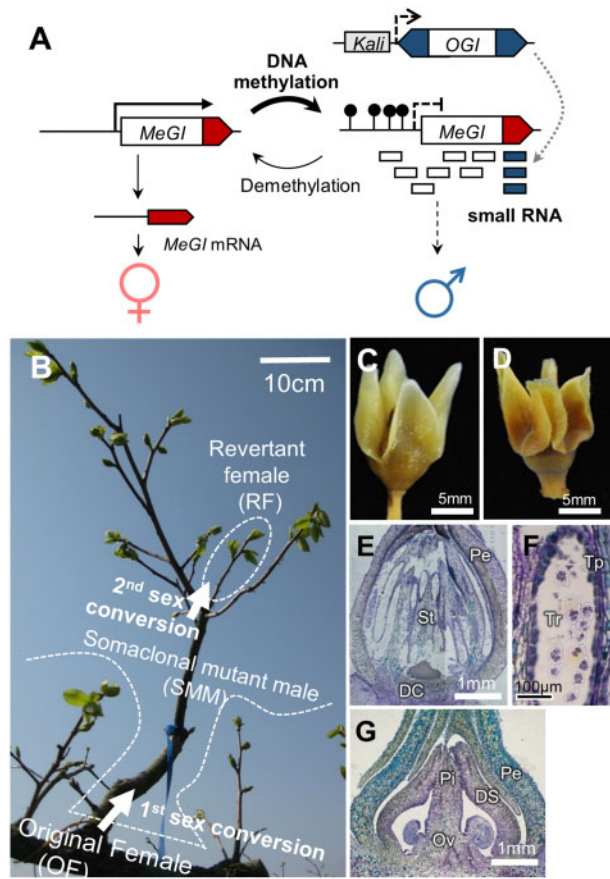
Fig. 1 Characterization of somaclonal sex conversions in persimmon. (A) Canonical system model for the formation of male flowers in hexaploid monoecious persimmon trees (Akagi et al. 2016a). Imperfectly silenced *OGI* is thought to trigger the accumulation of small RNAs targeting *MeGI* and the methylation of *MeGI*, ultimately leading to repressed *MeGI* expression and the production of male flowers. (B) Appearance of an SMM branch from a branch of a genetically female tree (OF) (first sex conversion) and an RF branch arising from an SMM branch (second sex conversion) in a persimmon tree (Saijo) grown in Shimane prefecture, Japan. Appearance of SMM (C) and RF (D) flowers at maturity (stage 3; Yang et al. 2019). Dissected SMM (E and F) and RF (G) flowers were stained with toluidine blue. The SMM flower bears intact stamens (St) and a deficient carpel (DC) (E). Image of SMM stamen at stage 3 and enclosed tetrads (TR) with a semi-mature tapetum cell layer (Tp) (F), which is consistent with normal male flowers in stage 3 (Yang et al. 2019). The RF flowers formed an intact pistil (Pi) and ovary (Ov), but a deficient stamen (DS) and no developing gametes, which is consistent with normal female flowers in stage 3.

and animal species (Tachibana 2016, Henry et al. 2018). For example, in melon (*Cucumis melo*), the conversion from male to female flowers in gynoecious lines results from epigenetic changes in the *CmWIP1* promoter (Martin et al. 2009). In *Silene* species, treating male plants with the demethylation agent 5-AzaC can induce hermaphroditism (Janousek et al. 1996) and Y alleles of the genes on the evolutionary stratum of the sex chromosomes are reportedly more highly methylated than the X alleles (Rodríguez Lorenzo et al. 2018). A recent study revealed that in *Populus balsamifera*, the epigenetic status of a candidate gene in the sex-determining region is highly

associated with the sex of flowers (Bräutigam et al. 2017). Regarding animals, some fish species have established an environment-based sex-determination system in which DNA methylation is essential (Shao et al. 2014). In mice, the gender-specific demethylation in the male liver is related to a postnatal pathway (Reizel et al. 2015). Despite these findings, the fundamental mechanisms underlying the regulation of epigenetic layers have been largely uncharacterized, especially in plants.

Long-lived (perennial) plants, especially vegetatively propagated tree crops, often produce visible somaclonal mutations (i.e. 'bud sports'). The mutant phenotypes may be maintained for at least a few years, but they occasionally revert back to the original phenotype, likely because of epigenetic regulation. In oil palm trees (*Elaeis guineensis*), the appearance of a somaclonally abnormal fruit type (i.e. mantled) is related to the decreased DNA methylation of transposons (Ong-Abdullah et al. 2015). In almond trees (*Prunus dulcis*), noninfectious bud failure is associated with clonal age and epigenetic status (Fresnedo-Ramírez et al. 2017). For both of these major tree crops, the appearance of altered phenotypes was thought to be mainly due to their long lives or long propagations. In addition, in the *D. kaki* cultivar Saijo, which lacks *OGI* and originally bears only female flowers, we detected somaclonal mutant male (SMM) branches and revertant female (RF) branches (**Fig. 1B–G**). This noncanonical male system, which does not involve *OGI*, has been observed in several independent Saijo trees in a specific area (Esumi et al. 2015), implying that epigenetic regulation contributes to this frequent sex conversion. Furthermore, the production of noncanonical male flowers has occasionally been observed in the cultivars Jiro and Fuyu, which also lack *OGI* (Yakushiji and Nakatsuka 2007, Akagi et al. 2014b). These findings suggest that certain epigenetic mutations to specific factors in genetically female individuals can induce noncanonical sex conversions in hexaploid persimmon species.

To characterize the mechanism underlying the production of noncanonical male flowers in a genetically female tree, we applied multi-omics approaches to examine early-stage flowers from the original female (OF), SMM and RF branches of Saijo trees. A comparison of the multitiered somaclonal mutations in an individual tree enabled us to elucidate the epigenetic regulation responsible for sex conversions and assess their potential contribution to gender gaps in persimmon. These insights may clarify the importance of the flexibility in epigenetic layers in a long-lived individual to overcome the genetic robustness of plants.

Results

Production of noncanonical male flowers on SMM branches depends on regulated *MeGI* expression

The canonical male flower production system in individuals carrying *OGI* depends on the accumulation of smRNAs targeting *MeGI* transcripts (sm*MeGI*), which substantially downregulates *MeGI* expression (**Fig. 1A**; Akagi et al. 2016a). To assess the possibility that *MeGI* expression patterns change during the sex
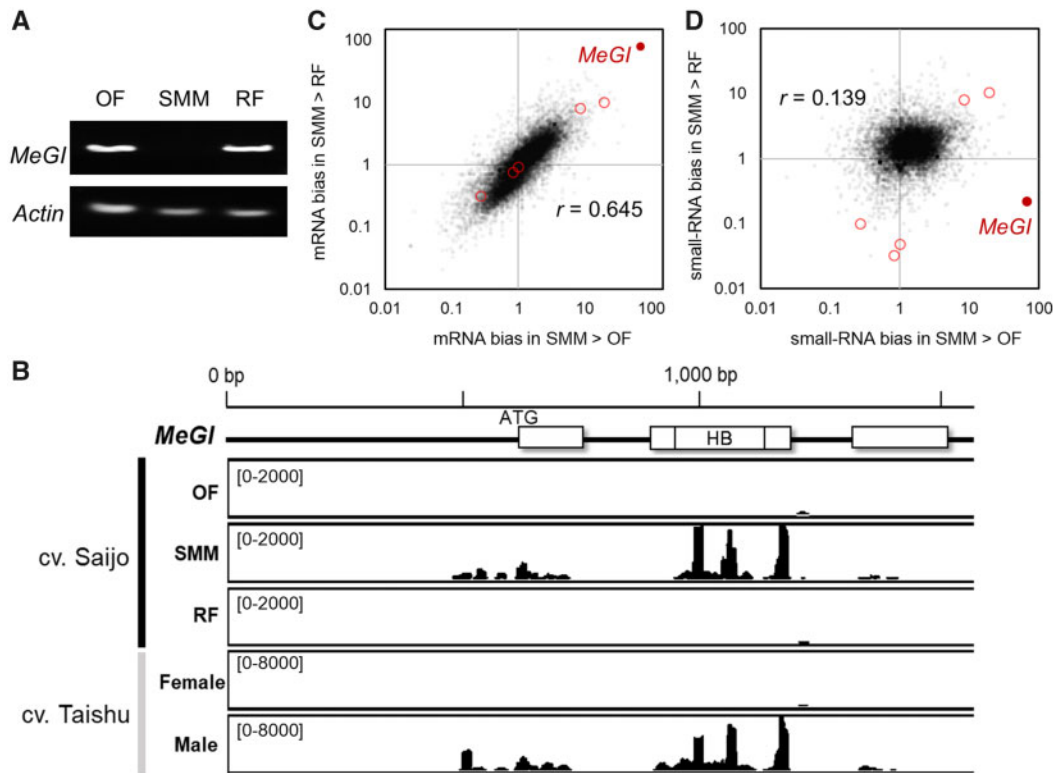
Fig. 2 SMM-specific downregulation of *MeGI* expression via the production of the noncanonical smRNAs targeting *MeGI*. (A) The *MeGI* expression level in early-stage flowers (stage 1; Yang et al. 2019) was assessed by qRT-PCR. The *Actin* gene served as the reference control. (B) Accumulation of smRNA across the *MeGI* gene and its promoter region in OF, SMM and RF flowers (stage 1) from Saijo trees and in normal male and female flowers from monoecious (canonical male-producing) Taishu trees. A substantial accumulation of smRNAs was observed in the male flowers of both cultivars, with a similar accumulation pattern. (C) Distribution of the smRNA expression biases between male and female flowers during the somaclonal sex conversions. The five DEGs between SMM and OF/RF flowers (RPKM >1) are highlighted in red. Of these DEGs, *MeGI* was associated with the highest and most consistent bias regarding the smRNA accumulation in the SMM and the female (OF and RF) flowers. (D) Distribution of the relationship between smRNA accumulation and mRNA expression in the comparison of SMM and the female (OF and RF) flowers. The five DEGs between SMM and OF/RF flowers are highlighted in red. Of these DEGs, *MeGI* specifically exhibited downregulated expression, with a considerable accumulation of smRNA.

conversions between SMM and OF/RF flowers, we analyzed flowers collected from OF, SMM and RF branches during the initial flower development stage (stage 1; Yang et al. 2019). We observed that the *MeGI* expression levels were much lower in the SMM flowers than in the two types of female flowers (**Fig. 2A**). These results suggested that changes in *MeGI* expression affect this noncanonical sex conversion.

We also conducted mRNA-Seq and smRNA-Seq analyses of early-stage OF, SMM and RF flowers to characterize the expression dynamics during the noncanonical sex conversions. Moreover, we compared the resulting data with that for the canonical male–female conversion in some monoecious cultivars carrying the *OGI* gene (Akagi et al. 2016a, Yang et al. 2019). The reads were mapped onto the reference genes of a diploid Caucasian persimmon species, *D. lotus* (DLO_r1.0; Akagi et al. 2019b), to calculate the expression levels as reads per kilobase per million reads (RPKM), filtering for substantially expressed genes (RPKM >1.0). smRNAs, especially 21- and 22-nucleotide smRNAs, targeting *MeGI* accumulated specifically in SMM flowers in the noncanonical system (**Supplementary Table S1**), which may involve the noncanonical RNA-dependent DNA methylation pathway and the action of Pol II and RDR6

(Matzke and Mosher 2014, Matzke et al. 2015), and the accumulation pattern was consistent with that in the canonical male production system (**Fig. 2B** and **Supplementary Table S1**). A comparison of the genome-wide smRNA surveys of the SMM flowers and the two female flowers (OF and RF) indicated that relatively few genes exhibited SMM-specific up- or downregulated expression. Moreover, the smRNA bias in the SMM/OF ratio was highly correlated with the smRNA bias in the SMM/RF ratio ($r = 0.65$; **Fig. 2C**). Only 20 genes exhibited a significantly enriched accumulation of smRNAs in an SMM-specific manner (>5-fold higher in SMM flowers than in female flowers, RPKM >10; **Supplementary Fig. S1** and **Supplementary Table S2**). These genes included *MeGI*, which was associated with the most biased smRNA accumulation in SMM flowers (SMM/OF = 67.7 and SMM/RF = 79.1; **Fig. 2C** and **Supplementary Fig. S1**).

An analysis of the mRNA-Seq data for early-stage flowers revealed 12 genes that were differentially expressed between the SMM flowers and the female flowers (OF and RF) according to the DESeq analysis (RPKM >1, $P < 0.1$; **Supplementary Fig. S2** and **Supplementary Table S3**). Of these genes, the expression levels of *MeGI* and *AGL6*, which encode transcription

factors, were significantly downregulated in SMM flowers ($P = 0.012$ and 0.053, respectively), which is consistent with their expression patterns in canonical male flowers (Yang et al. 2019). The smRNA-Seq and mRNA-Seq analyses suggested that the smRNA-dependent regulation of *MeGI* expression is responsible for the sex conversion between SMM and female (OF or RF) flowers in the noncanonical system as well as in the canonical system. Furthermore, among the differentially expressed genes (DEGs) between SMM and OF/RF flowers, only *MeGI* was associated with a substantial accumulation of smRNAs (**Fig. 2D**), which is also consistent with the canonical sex-determination system (Akagi et al. 2016a). These observations suggested that the biased accumulation of trans-acting smRNAs has little effect on sex differentiation in canonical and noncanonical systems.

DNA methylation of the *MeGI* promoter in the noncanonical male production system

The accumulation of the smRNAs targeting *MeGI* is highly associated with how extensively the *MeGI* promoter is methylated (Akagi et al. 2016a). In the current study, we conducted a bisulfite PCR-Seq analysis of the 300-bp 5' *MeGI* promoter region in the early-stage flower buds and leaves to determine the DNA methylation levels in the SMM and OF/RF (defined as 'mutated branch'), in the other branches in the same tree, and in other trees of the same cultivar, as well as in the canonical male-producing cultivars carrying the *OGI* gene. The weighted DNA methylation level in SMM flowers was 8.0%, which was significantly higher than that of OF or RF flowers (0.6% and 0.5%, respectively, $P < 2.2e^{-16}$ and $<2.2e^{-16}$ with Fisher's exact test, respectively; **Fig. 3A**). These results were indicative of an association between the methylation levels in the

MeGI promoter and the OF–SMM–RF sex conversions. The methylation levels of all three contexts (CGN, CHG and CHH) were substantially higher in SMM flowers than in the OF and RF flowers (**Fig. 3A** for the average and **Supplementary Fig. S3A–C** for each residue). These SMM-specific higher DNA methylation levels were consistent with the difference between male and female in the canonical system of a monoecious cultivar, Taishu (**Supplementary Fig. S3E, F**). Furthermore, the DNA methylation levels for OF and RF (both female) flowers collected from trees grown in Shimane prefecture (35.47°N, 132.85°E) were slightly but significantly higher than those of a hypotetically identical cultivar, Saijo, grown in the experimental orchard of Kyoto University (35.03°N, 135.79°E; **Fig. 3** and **Supplementary Figs. S3D, S4** for test of genetic identity of them; Onoue et al. 2018). The DNA methylation in the other branches of the mutated Saijo and other Saijo trees in the same orchard also showed the tendency of higher methylation in *MeGI* in comparison to the Saijo tree in Kyoto (**Supplementary Fig. S5A**). Similar to the DNA methylation pattern in flower buds, leaves also showed higher DNA methylation in SMM-specific manner, although their methylation levels were quite lower than those in flowers (**Fig. 3B**; 0.60% for SMM, while 0.40% and 0.45% for OF and RF with $P < 2.2e^{-16}$ and $<2.2e^{-16}$ for Fisher's exact test against SMM, respectively). The CGN and CHG contexts showed clear differences in comparison of SMM and OF/RF, while the CHH methylation showed only slight (but statistically significant) differences ($p = 6.5e^{-9}$ and 0.001, respectively; **Fig. 3B** and **Supplementary Fig. S5B**). In monoecious cultivars, the DNA methylation of the *MeGI* promoter is critical for the maintenance of smRNA accumulation. The DNA methylation level for maintaining or releasing smRNAs varies between cultivars, with independent threshold levels, as revealed in a
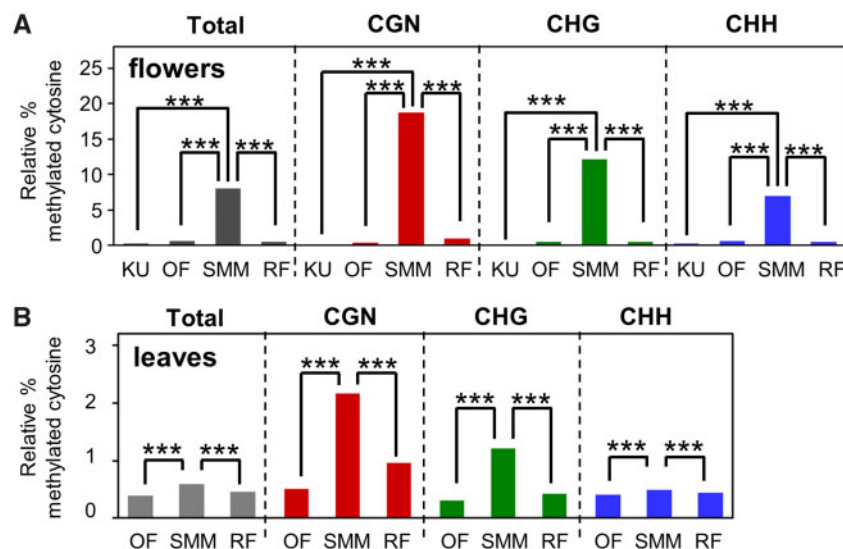

Fig. 3   DNA methylation of the *MeGI* promoter in flowers and leaves during the noncanonical sex conversion. The DNA methylation levels in the *MeGI* 5' promoter region (300 bp from the start codon) in the three contexts (CGN, CHG and CHH), in early flower developing stage (stage 1, Yang et al. 2019) (A) and in young leaves (B). The DNA methylation levels were substantially higher in SMM flowers on all the three contexts than those in OF/RF flowers from Saijo trees grown in Shimane prefecture. This tendency was consistent with the DNA methylation levels in leaves in comparison of OF–SMM–RF, in all three contexts, although the biases were fundamentally smaller than in flowers. In comparison of female flowers, the methylation levels in OF and RF were significantly higher than in female flowers from Saijo trees planted at Kyoto University (KU). This tendency was consistent with the DNA methylation levels in leaves in comparison of OF–SMM–RF, in all three contexts, although the biases were fundamentally smaller than in flowers. Bars indicate SE, ***$P < 0.001$.

previous study involving treatments with DNA demethylation agents (Akagi et al. 2016a). Our results were suggestive of the possibility that the more extensive DNA methylation of the *MeGI* promoter in SMM than in OF and RF with branch unit resulted in an SMM-specific smRNA accumulation, consistent with the canonical system.

Genome-wide comparison of DNA methylation levels during somaclonal sex conversions

To assess the genome-wide tendencies of DNA methylations in OF, SMM and RF flowers, we analyzed the DNA methylomes by whole-genome bisulfite sequencing with DNA from early-stage OF, SMM and RF flowers as the template. We calculated the

methylation levels in four contexts (CGN, CGH, CHH and total; read coverage >10; **Supplementary Table S4** for the metrics of whole-genome bisulfite sequencing). Genome-wide analyses revealed 13,840 CGN, 31,037 CHG and 147,532 CHH contexts. To characterize the differentially methylated regions in the persimmon genome among SMM and OF/RF samples, we calculated the weighted methylation levels with 500-kb bin windows in the whole genome (**Fig. 4A–D**) and within the 1,000-bp segments flanking gene bodies (**Fig. 4E–G**; read coverage >5). The CGN and CHG sequences exhibited SMM-enriched methylation levels relative to the OF ($P = 3.1e^{-123}$ for CGN and $P = 3.2e^{-20}$ for CHG, respectively) and RF levels ($P = 1.5e^{-313}$ for CGN and $P = 9.0e^{-61}$ for CHG, respectively) according to
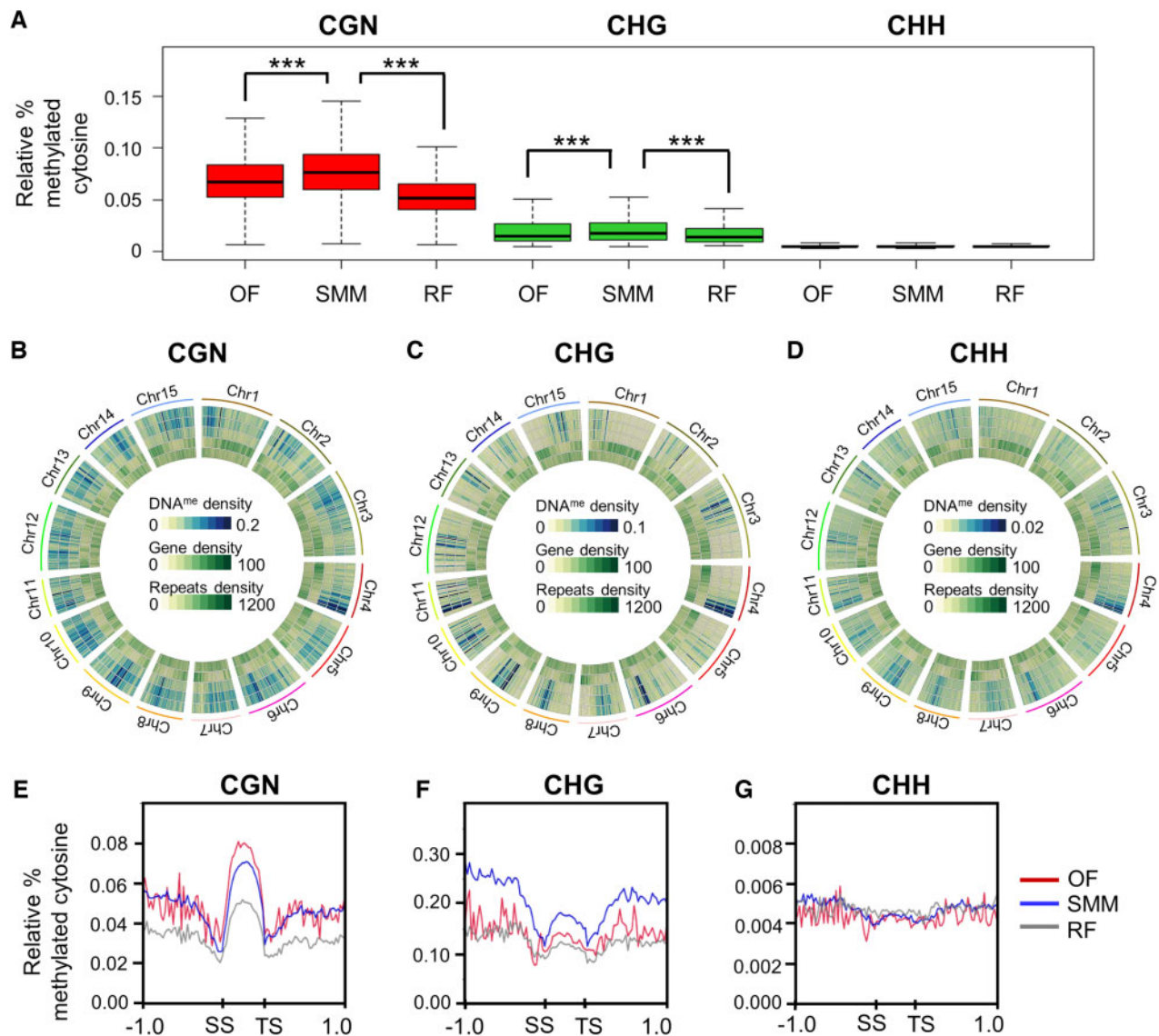

Fig. 4 Changes to genome-wide DNA methylation during the noncanonical sex conversions. (A) Average whole-genome DNA methylation levels in all three contexts. Each context was given in red, green and blue. Bars indicate SE. ***P < 0.001. Distribution of DNA methylation levels in the three contexts [CGN (B), CHG (C) and CHH (D)]. From the outer layer, DNA methylation levels in 500-kb bin in OF (1), SMM (2) and RF (3) and the densities of genes (4) and repetitive regions (5) were given. DNA methylation levels were significantly higher in the SMM, on CGN and CHG in genome-wide, remarkably on repetitive regions. DNA methylation levels in 50-bp bins of the gene bodies and in the 1,000-bp flanking regions in the CGN (E), CHG (F) and CHH (G) contexts. Data for the OF, SMM and RF flowers are presented in red, blue and gray, respectively. SS, start site (start codon); TS, termination site (stop codon).

the paired *t*-test. In addition, the methylation levels were significantly higher in OF flowers than in RF flowers ($P = 4.6e^{-216}$ for CGN and $P = 2.4e^{-29}$ for CHG; **Fig. 4A**). The genome-wide tendencies also indicated that SMM-enriched CGN and CHG methylations were observed on both genes and repetitive regions (**Fig. 4B, C**). These methylation-level tendencies were consistent with the relative DNA methylation levels for the *MeGI* gene in the SMM, OF and RF flowers and leaves (**Fig. 3**). However, there were no significant differences in the genome-wide CHH methylation level in the three flower types ($P = 0.65$ for OF vs. SMM and 0.76 for RF vs. SMM; **Fig. 4A, D**). These results implied that the male-specific greater methylation in the CGN and CHG contexts might be associated with the noncanonical male production system.

Our bin analysis of methylation levels surrounding complete genes indicated that the CHG context exhibited an SMM-specific enrichment of methylation both in the gene body and in the flanking regions (**Fig. 4F**). In contrast, there were no significant differences in the methylation of the CGN context in the OF and SMM flowers, whereas the methylation level decreased in the transition from SMM to RF flowers (**Fig. 4E**). The CHH context was similarly methylated in the three flower types (**Fig. 4G**). Thus, the DNA methylation levels of the gene bodies and flanking regions were consistent with the genome-wide methylation patterns, with only some inconsistencies (e.g. CGN context of SMM and OF flowers).

We also assessed the correlation between relative methylation levels and mRNA/smRNA expression levels. The DNA methylation patterns for the 5′ 1-kb promoters and gene bodies were not associated with mRNA and smRNA dynamics (3,860 methylated genes; read coverage >50) in the female (OF and RF) and SMM flowers (**Fig. 5A–C** and D–F for the DNA methylation of the
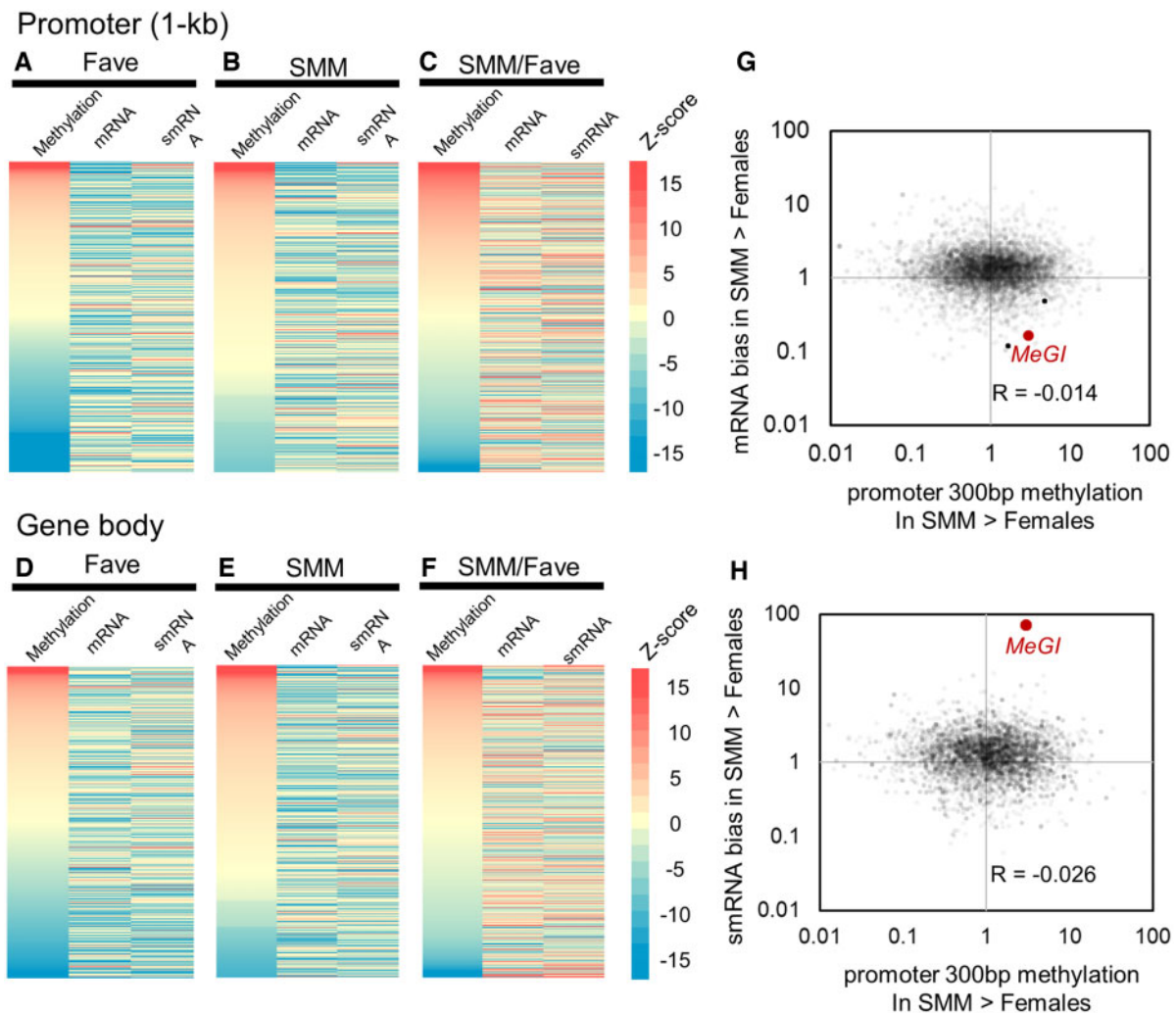

Fig. 5 Correlation between DNA methylation and mRNA/smRNA expression levels. Heatmap visualization of the correlations between mRNA/smRNA expression levels and relative DNA methylation levels of the 5′ 1-kb promoters (A–C) or in the gene bodies (D–F). Data are provided for the average OF/RF flower (Fave), SMM flower and the SMM/Fave ratio. The methylation and expression levels are indicated as standardized values across the genes. No clear correlations ($r < 0.1$) and tendencies were observed between the genome-wide DNA methylation and gene expression levels. Genome-wide distribution of the DNA methylation and mRNA (G) or smRNA (H) biases between Fave and SMM flowers. The DNA methylation biases in Fave and SMM flowers were correlated with the expression levels of specific genes (e.g. *MeGI*), but not with the genome-wide gene (or smRNA) expression levels.

promoter regions and gene bodies, respectively). Furthermore, the DNA methylation biases in the promoter regions of the SMM and female (OF and RF) flowers were not significantly correlated with the mRNA (**Fig. 5G**, $r = -0.014$) or smRNA (**Fig. 5H**, $r = -0.026$) expression biases. The DNA methylation and mRNA or smRNA expression levels were consistent for only a part of genes, such as *MeGI*, on all three contexts (CGN, CHG and CHH; **Fig. 5G,H**, **Supplementary Table S5** and **Supplementary Fig. S6**). Although the average DNA methylation levels were substantially lower in the OF and RF flowers than in the SMM flowers (**Fig. 4A**), the methylation patterns varied between OF and RF flowers, especially regarding the gene bodies (**Supplementary Fig. S7**). Therefore, the methylation patterns clearly linked to sex determination may be limited to specific genes, such as *MeGI* (**Supplementary Fig. S8** for the summarized information of mRNA, smRNA and DNA methylation patterns in OF–SMM–RF).

Discussion

Our results presented herein suggest that the noncanonical male production system fundamentally shares a regulatory pathway with the canonical system, which depends on the *OGI* gene, where sex conversions are associated with the epigenetic regulation of *MeGI*, given in a model (**Fig. 6**). In this model, the *MeGI* methylation level might be coordinated with the genome-wide fluctuation in DNA methylation, although there are still issues for this link, described later. The SMM-specific hypermethylation was specific to the mutated 'branch' unit (**Fig. 3** and **Supplementary Fig. S5**), which was not

conserved in the surrounding trees even in the same cultivar, whereas the basic methylation level in the objective region (or orchard) was significantly higher than in Saijo in Kyoto (**Fig. 3** and **Supplementary Fig. S5**). This situation might explain the frequent appearance of mutant male branches in Saijo in Shimane prefecture (Esumi et al. 2015), which is supported by the fact that, even in a small range, the *MeGI* methylation exceeding the cultivar-dependent threshold induced the accumulation of small-*MeGI* and the resultant production of male flowers (Akagi et al. 2016a). Regarding the environmental factors involved in this situation, empirical knowledge concerning the cultivation of persimmon trees suggests that young and vigorous plants (or branches) tend to produce more female flowers, which may support the possibility that a genome-wide epigenetic status in plants affects *MeGI* methylation. Considerable epigenetic flexibility in long-lived plants, or in trees, is often associated with long vegetative propagation (Bräutigam et al. 2013). In persimmon, the Saijo tree bearing SMM branch has been maintained for approximately 20 years after the grafting of young scions. On the other hand, the Saijo tree in Kyoto, which has been maintained for >50 years, has so far not exhibited any sex conversions. This suggests that plant age alone cannot explain the epigenetic flexibility and resulting sex conversion in persimmon.

The DNA methylation in *MeGI* was significantly changed in all three contexts, CGN, CHG and CHH, between SMM and females (OF and RF), whereas potentially coordinated genome-wide DNA methylation showed fundamental changes only in CGN or CHG. This difference in the methylated contexts between in *MeGI* and at whole-genome might be a clue for the
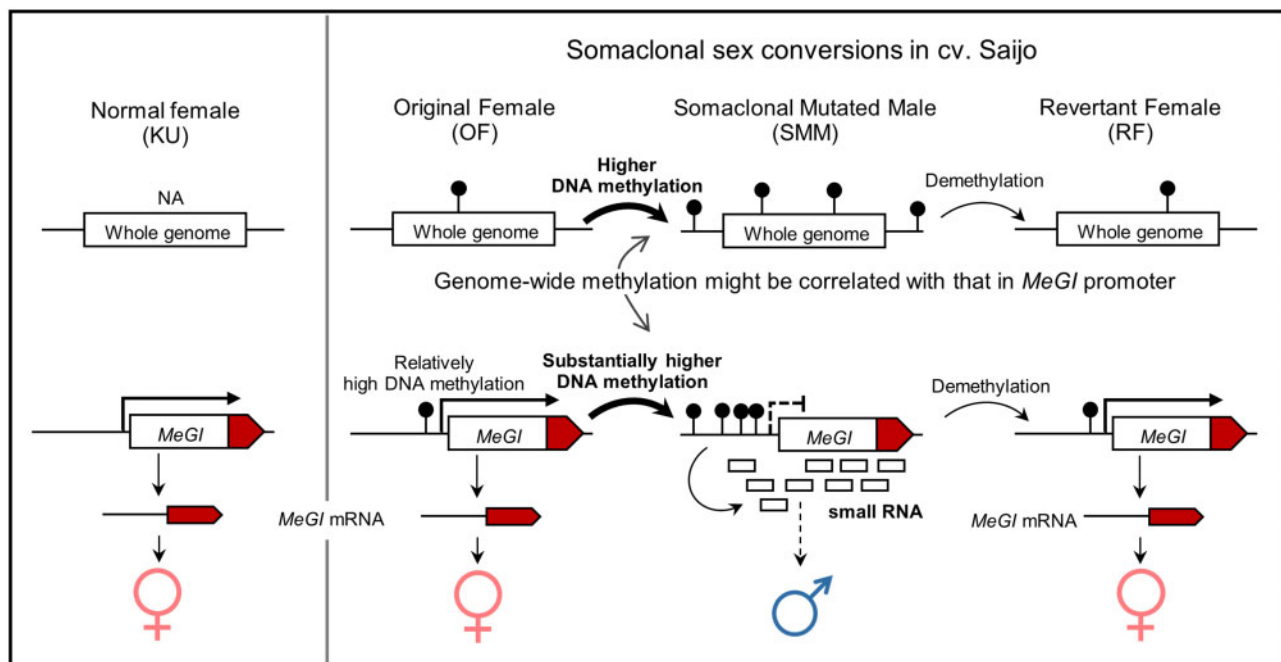

Fig. 6 Model for the noncanonical sex conversion system in a genetically female persimmon tree. The basic methylation levels in Saijo trees in the region including the mutated tree might be slightly higher than those in normal Saijo tree. Noncanonical sex conversions are associated with the epigenetic changes to *MeGI*, which might be coordinated with the genome-wide DNA methylation tendencies during the transition to and from male flowers. This change in DNA methylation to derive male branch occurred in a branch unit.

mechanism of this somaclonal conversion to male. Among the representative genes involving maintenance of DNA methylation (Matzke and Mosher 2014), the expression of a DNA methyltransferase specific to CHH, CMT2, was slightly biased to SMM (>1.2-fold higher in SMM flowers than in female flowers, RPKM >1; **Supplementary Table S6**), although the difference is not statistically significant ($p > 0.5$). From a viewpoint of environmental signals, the CHH type of demethylation was the major response to low temperature in the cucumber, which promotes femaleness (Lai et al. 2017). CMT2 has been found to be associated with temperature seasonality in Arabidopsis in a genome-wide association analysis (Shen et al. 2014). Furthermore, *cmt2* mutant plants have heat stress tolerance, suggesting that CMT2-dependent CHH methylation may act as an important alleviator of heat stress responses (Shen et al. 2014). The substantially lower temperature in Shimane than in Kyoto during flower differentiation from May to September in 2014–2015, when the mutant male flowers were first differentiated (**Supplementary Table S7**, Japan Meteorological Agency), might also be involved in the differences in DNA methylation levels. Although only limited environmental variants would not be able to explain the frequent appearance of noncanonical male flowers, future testing with potted plants would allow identifying environmental factors affecting the change in DNA methylation and noncanonical sex conversions.

Although the epigenetic status of *MeGI* dramatically affected its expression pattern and the resulting sex of flowers, most of the genes in the genome were insensitive to the epigenetic variations between male and female flowers, at least regarding smRNA accumulation (**Fig. 2D**) and DNA methylation (**Fig. 5**). In contrast to mutants associated with abnormal DNA methylation, such as *met1* (Kankel et al. 2003, Chan et al. 2006), the natural variations in the methylation status of the *Arabidopsis thaliana* genome may explain the relatively few examples of expression-level changes and features in diverse accessions (Kawakatsu et al. 2016). Similarly, despite the considerable epigenetic flexibility in an individual, our results imply that sex-specific epigenetic variations can regulate the expression of only some genes in persimmon flowers. Future investigations of the genome-wide DNA methylation patterns in various cultivars (or genotypes) may provide deeper insights into the importance of epigenetic variations in long-lived persimmon trees.

Materials and Methods

Plant materials

Flower buds and leaves on the OF, SMM and RF branches of the hexaploid *D. kaki* cv. Saijo trees grown in Shimane prefecture, Japan ($35.47°$N, $132.85°$E), were harvested on April 4, 2018, which corresponds to the early developmental stage before organs differentiated (Akagi et al. 2016a). Normal male or female flower buds from Taishu and Saijo trees grown in the experimental orchard of Kyoto University were harvested during the same developmental stage (April 1–5, 2015 and 2016). Normal female flower buds and leaves from other branches in the mutated tree and other trees of the same cultivar, Saijo in the orchard, where the mutated branch was found, were harvested on April 9, 2019. The collected samples were frozen at $-80°$C until used for DNA/RNA extractions.

PCR expression analysis

Total RNA was extracted from the collected flower samples with the PureLink® Plant Reagent (Invitrogen, USA) and then purified by a phenol/chloroform

extraction. First-strand cDNA was synthesized with the ReverTra Ace® qPCR RT Master Mix (Toyobo, Japan) for a subsequent analysis of *MeGI* expression by PCR (**Supplementary Table S4**). The constitutively expressed *DkActin* gene was used for standardizing the expression levels (Akagi et al. 2019a, Akagi et al. 2019b).

Preparation and sequencing of mRNA-Seq and smRNA-Seq libraries

To construct mRNA-Seq libraries, total RNA was purified with the Dynabeads mRNA Purification Kit (Invitrogen, USA). Illumina sequencing libraries were prepared with the KAPA HyperPrep Kit (Roche, Switzerland) as previously described (Yang et al. 2019). Thirteen cycles of PCR enrichment were completed, followed by a DNA cleanup step with AMPure XP beads (AMPure:reaction = 0.8:1; Beckman Coulter, USA). The constructed libraries were sequenced with the HiSeq 4000 system (50-bp single-end reads; Illumina).

To construct smRNA-Seq libraries, the smRNA fraction was isolated from total RNA and concentrated with the mirVana miRNA Isolation Kit (Life Technology, USA). Approximately 200 ng of concentrated smRNA was used to construct the libraries with the NEBNext Small RNA Library Prep Set (NEB, USA) as previously described (Akagi et al. 2016a). Fifteen cycles of PCR enrichment were completed, followed by a DNA cleanup step with AMPure (AMPure:reaction = 1.1:1) to remove self-ligated adapter dimers. The constructed libraries were sequenced with the HiSeq 4000 system (50-bp single-end reads).

The Illumina sequencing was conducted at the Vincent J. Coates Genomics Sequencing Laboratory at UC Berkeley, USA. The raw sequencing reads were processed with custom Python scripts developed in the Comai laboratory (**http://comailab.genomecenter.ucdavis.edu/index.php/Barcoded_data_preparation_tools**) as previously described (Akagi et al. 2014a). Briefly, reads were split based on the index information and trimmed for quality (Phred sequence quality >20 over a 5-bp sliding window) and to eliminate adapter sequence contamination. Reads <35 and <19 bp were excluded from the mRNA-Seq and smRNA-Seq analyses, respectively.

Expression profiling

The mRNA-Seq and smRNA-Seq reads were aligned to the reference coding sequences of the diploid Caucasian persimmon species *D. lotus* (Akagi et al. 2019a, Akagi et al. 2019b) with the default parameters of the Burrows–Wheeler Aligner (version 0.7.12; **https://github.com/lh3/bwa**; Li and Durbin 2009). The read counts per coding sequence were generated from the aligned SAM files with a custom R script (Akagi et al. 2016a) to calculate the normalized gene expression levels. For the mRNA-Seq data, the DEGs between OF/RF and SMM flowers were detected by a DESeq analysis (sharing mode = fit-only; Robinson et al. 2010). The DEGs were further filtered based on RPKM and FDR values (RPKM >1.0 and FDR <0.1). Putative functions of each gene were assigned according to a BLASTX search of the TAIR10 database (**http://www.arabidopsis.org/index.jsp**).

Bisulfite PCR-Seq analysis

Genomic DNA was extracted from young flower buds with the cetyltrimethylammonium bromide method (Akagi et al. 2014b) or DNeasy Plant Mini Kit (Qiagen, Netherlands), after which it was treated with the EZ DNA Methylation-Gold kit (Zymo Research, USA) to deaminate and convert non-methylated cytosine residues into uracil residues. Bisulfite-treated *MeGI* promoter sequences were amplified with Epi Taq HS (Takara Bio Inc, Japan) and specific sense- and antisense-direction primer sets (**Supplementary Table S8**). The amplicons were subjected to an end-repair step, after which an A-base overhang and an adapter were added as described in the mRNA Illumina libraries construction section. Five cycles of PCR enrichment were completed, followed by a DNA cleanup step with AMPure (AMPure:reaction = 0.7:1). The constructed libraries were sequenced with the HiSeq 4000 system (150-bp paired-end reads). The forward and reverse reads of the bisulfite PCR-Seq data were separately mapped to the 5′ promoter region of the *MeGI* gene as described and then analyzed with the Methylpy program (**https://github.com/yupenghe/methylpy**) to determine the DNA methylation levels as described by Kawakatsu et al. (2016). Only residues with a coverage of >20 were used for analyzing DNA methylation. The samples harvested in 2019 were conducted for the bisulfite sequencing of only

sense sequence as the index. The significances of DNA methylation levels between samples were calculated with Fisher's exact test.

Fragment size analysis for the identification of the cultivar Saijo

Multiplex PCR of the AST locus-linked region was performed with two fluorescent-labeled forward primers HEX-AST-F and FAM-PCNA-F and unlabeled reverse primer 5R3R (Kanzaki et al. 2010; Supplementary Table S8). The 10-μl PCR mixture contained 5 μl of PrimeSTAR MAX (Takara), 0.2 μM of primers and 10–20 ng of genomic DNA. The PCR conditions were as follows: 95 C for 3 min, followed by 27 cycles at 95 C for 30 s, 55 C for 30 s, 72 C for 1 min and final extension at 72 C for 10 min. The amplified PCR products were separated by ABI 3730XL (Thermo Fisher Scientific Inc.). The size of each amplified fragment was calculated based on the 350 Dye Size Standard by PeakScanner ver. 1.0 (Thermo Fisher Scientific Inc.).

MethylC-Seq analysis

The MethylC-Seq libraries were prepared with genomic DNA extracted from flower buds as previously described (Urich et al. 2015). Briefly, DNA was fragmented to 350-bp segments, followed by an end-repair step and the addition of an adenosine tail and an adapter. The resulting adapter-ligated DNA was isolated by two rounds of purification with AMPure XP beads (200–600 bp) and then subjected to a bisulfite conversion with the EZ DNA Methylation-Gold kit. The bisulfite-converted DNA molecules were enriched by four cycles of PCR. The amplicons were purified using AMPure (AMPure:reaction = 1:1). The methylC-Seq libraries were sequenced with the HiSeq 4000 system (100-bp paired-end reads). The MethylC-Seq reads were divided into two groups (forward and reverse reads) and then mapped to the primary genomic scaffold sequences of diploid *D. lotus* (Akagi et al. 2019a, Akagi et al. 2019b) with the Methylpy program. Genome-wide DNA methylation levels were calculated as methylated residues/filtered read count with coverage >10 within 500-kb bin. The DNA methylation was visualized using the circos plot program as described by Kawakatsu et al. (2016). The DNA methylation levels for gene bodies and the 1,000-bp regions flanking the coding sequences were visualized using the deepTools program (https://deeptools.readthedocs.io/en/develop/). The data in the read count files were filtered (coverage >5) and separated based on the DNA methylation contexts (CGN, CHG and CHH). The DNA methylation levels on gene bodies and flanking regions were calculated with Compute Matrix and visualized using the plotProfile program of deepTools as described by Kawakatsu et al. (2016).

Correlation between DNA methylation and expression levels

The genome-wide methylation patterns in the 5′ 1-kb promoters and gene bodies were calculated as previously described by Kawakatsu et al. (2016). The methylated cytosines of all three contexts (CGN, CHG and CHH) in the promoters and gene bodies were extracted from the read count file with a custom Python script and the generic feature format (gff) file of the diploid *D. lotus* (Akagi et al. 2019a, Akagi et al. 2019b). The methylation patterns were calculated as methylated residues/filtered read count with coverage >50. The correlation between the methylation patterns and mRNA/smRNA expression levels was calculated based on the Pearson correlation analysis. The data for the methylation patterns were combined with the filtered mRNA and smRNA data (RPKM >1). The combined data were standardized based on the Z-score and visualized with a heatmap. The relationships between the 300-bp promoter methylation bias in SMM/female flowers with the mRNA bias and smRNA bias in SMM/female flowers were visualized with plotted figures.

Supplementary Data

Supplementary data are available at PCP online.

References

Ainsworth, C. (2000) Boys and girls come out to play: the molecular biology of dioecious plants. *Ann. Bot.* 86: 211–221.

Akagi, T., Henry, I.M., Kawai, T., Comai, L. and Tao, R. (2016a) Epigenetic regulation of the sex determination gene *MeGI* in polyploid persimmon. *Plant Cell* 28: 2905–2915.

Akagi, T., Henry, I.M., Ohtani, H., Morimoto, T., Beppu, K., Kataoka, I., et al. (2018) A Y-encoded suppressor of feminization arose via lineage-specific duplication of a cytokinin response regulator in Kiwifruit. *Plant Cell* 30: 780–795.

Akagi, T., Henry, I.M., Tao, R. and Comai, L. (2014a) A Y-chromosome-encoded small RNA acts as a sex determinant in persimmons. *Science* 346: 646–650.

Akagi, T., Kajita, K., Kibe, T., Morimura, H., Tsujimoto, T., Nishiyama, S., et al. (2014b) Development of molecular markers associated with sexuality in *Diospyros lotus* L. and their Application in *D. kaki* Thunb. *J. Jpn. Soc. Hortic. Sci.* 83: 214–221.

Akagi, T., Kawai, T. and Tao, R. (2016b) A male determinant gene in diploid dioecious *Diospyros*, *OGI*, is required for male flower production in monoecious individuals of Oriental persimmon (*D. kaki*). *Sci. Hortic.* 213: 243–251.

Akagi, T., Pilkington, S.M., Varkonyi-Gasic, E., Henry, I.M., Sugano, S.S., Sonoda, M., et al. (2019a) Two Y-chromosome-encoded genes determine sex in kiwifruit. *Nat. Plants* 5: 801–809.

Akagi, T., Shirasawa, K., Nakazaki, H., Hirakawa, H., Tao, R., Comai, L., et al. (2019b) The persimmon genome reveals clues to the evolution of a lineage-specific sex determination system in plants. bioRxiv, doi: 10.1101/628537.

Bräutigam, K., Soolanayakanahally, R., Champigny, M., Mansfield, S., Douglas, C., Campbell, M.M., et al. (2017) Sexual epigenetics: gender-specific methylation of a gene in the sex determining region of *Populus balsamifera*. *Sci. Rep.* 7: 1–8.

Bräutigam, K., Vining, K.J., Lafon-Placette, C., Fossdal, C.G., Mirouze, M., Marcos, J.G., et al. (2013) Epigenetic regulation of adaptive responses of forest tree species to the environment. *Ecol. Evol.* 3: 399–415.

Chan, S.W.L., Henderson, I.R., Zhang, X., Shah, G., Chien, J.S.C. and Jacobsen, S.E. (2006) RNAi, DRD1, and histone methylation actively target developmentally important Non-CG DNA methylation in *Arabidopsis*. *PLoS Genet.* 2: e83–797.

Esumi, T., Watanabe, A., Kosugi, Y., Ohata, K. and Itamura, H. (2015) Staminate flowers on 'Saijo' persimmon (*Diospyros kaki* Thunb.). *Bull. Fac. Life Environ. Sci. Shimane Univ.* 20: 3–8.

Fresnedo-Ramírez, J., Chan, H.M., Parfitt, D.E., Crisosto, C.H. and Gradziel, T.M. (2017) Genome-wide DNA-(de)methylation is associated with Noninfectious Bud-failure exhibition in Almond (*Prunus dulcis* [Mill.] D.A.Webb). *Sci. Rep.* 7: 1–12.

Harkess, A., Zhou, J., Xu, C., Bowers, J.E., Van Der Hulst, R., Ayyampalayam, S., et al. (2017) The asparagus genome sheds light on the origin and evolution of a young Y chromosome. *Nat. Commun.* 8: 1279.

Hartwig, T., Chuck, G.S., Fujioka, S., Klempien, A., Weizbauer, R., Potluri, D.P. V., et al. (2011) Brassinosteroid control of sex determination in maize. *Proc. Natl. Acad. Sci. U. S. A.* 108: 19814–19819.

Henry, I.M., Akagi, T., Tao, R. and Comai, L. (2018) One hundred ways to invent the sexes: theoretical and observed paths to dioecy in plants. *Annu. Rev. Plant Biol.* 69: 553–575.

Janousek, B., Siroky, J. and Vyskot, B. (1996) Epigenetic control of sexual phenotype in a dioecious plant. *Mol. Gen. Genet.* 250: 483–490.

Kankel, M.W., Ramsey, D.E., Stokes, T.L., Flowers, S.K., Haag, J.R., Jeddeloh, J.A., et al. (2003) Arabidopsis *MET1* cytosine methyltransferase mutants. *Genetics* 163: 1109–1122.

Kanzaki, S., Akagi, T., Masuko, T., Kimura, M., Yamada, M., Sato, A., et al. (2010) SCAR markers for practical application of marker-assisted selection in persimmon (*Diospyros kaki* Thunb.) breeding. *J. Jpn. Soc. Hortic. Sci.* 79: 150–155.

Kawakatsu, T., Huang, S., Shan, C., Jupe, F., Sasaki, E., Schmitz, R.J.J., Urich, M. A.A., et al. (2016) Epigenomic diversity in a global collection of *Arabidopsis thaliana* accessions. *Cell* 166: 492–506.

Lai, Y., Zhang, X., Zhang, W., Shen, D., Wang, H., Xia, Y., Qiu, Y., et al. (2017) The association of changes in DNA methylation with temperature-dependent sex determination in cucumber. *J. Exp. Bot.* 68: 2899–2912.

Li, H. and Durbin, R. (2009) Fast and accurate short read alignment with Burrows-Wheeler transform. *Bioinformatics* 25: 1754–1760.

Martin, A., Troadec, C., Boualem, A., Rajab, M., Fernandez, R., Morin, H., et al. (2009) A transposon-induced epigenetic change leads to sex determination in melon. *Nature* 461: 1135–1138.

Matzke, M.A., Kanno, T. and Matzke, A.J. (2015) RNA-directed DNA methylation: the evolution of a complex epigenetic pathway in flowering plants. *Annu. Rev. Plant Biol.* 66: 243–267.

Matzke, M.A. and Mosher, R.A. (2014) RNA-directed DNA methylation: an epigenetic pathway of increasing complexity. *Nat. Rev. Genet.* 15: 394–408.

Ming, R., Bendahmane, A. and Renner, S.S. (2011) Sex chromosomes in land plants. *Annu. Rev. Plant Biol.* 62: 485–514.

Murase, K., Shigenobu, S., Fujii, S., Ueda, K., Murata, T., Sakamoto, A., et al. (2017) MYB transcription factor gene involved in sex determination in *Asparagus officinalis*. *Genes Cells* 22: 115–123.

Ong-Abdullah, M., Ordway, J.M., Jiang, N., Ooi, S.-E., Kok, S.-Y., Sarpan, N., et al. (2015) Loss of *Karma* transposon methylation underlies the mantled somaclonal variant of oil palm. *Nature* 525: 533–537.

Onoue, N., Kobayashi, S., Kono, A. and Sato, A. (2018) SSR-based molecular profiling of 237 persimmon (*Diospyros kaki* Thunb.) germplasms using *ASTRINGENCY*-linked marker. *Tree Genet. Genomics* 14: 1–18.

Reizel, Y., Spiro, A., Sabag, O., Skversky, Y., Hecht, M., Keshet, I., et al. (2015) Gender-specific postnatal demethylation and establishment of epigenetic memory. *Genes Dev.* 29: 923–933.

Renner, S.S. (2014) The relative and absolute frequencies of angiosperm sexual systems: dioecy, monoecy, gynodioecy, and an updated online database. *Amer. J. Bot.* 101: 1588–1596.

Robinson, M.D., McCarthy, D.J. and Smyth, G.K. (2010) edgeR: a Bioconductor package for differential expression analysis of digital gene expression data. *Bioinformatics* 26: 139–140.

Rodríguez Lorenzo, J.L., Hobza, R. and Vyskot, B. (2018) DNA methylation and genetic degeneration of the Y chromosome in the dioecious plant *Silene latifolia*. *BMC Genomics* 19: 8.

Shao, C., Li, Q., Chen, S., Zhang, P., Lian, J., Hu, Q., et al. (2014) Epigenetic modification and inheritance in sexual reversal of fish. *Gen. Res.* 24: 604–615.

Shen, X., De Jonge, J., Forsberg, S.K.G., Pettersson, M.E., Sheng, Z., Hennig, L., et al. (2014) Natural CMT2 variation is associated with genome-wide methylation changes and temperature seasonality. *PLoS Genet.* 10: e1004842–14.

Tachibana, M. (2016) Epigenetics of sex determination in mammals. *Reprod. Med. Biol.* 15: 59–67.

Tsugama, D., Matsuyama, K., Ide, M., Hayashi, M., Fujino, K. and Masuda, K. (2017) A putative *MYB35* ortholog is a candidate for the sex-determining genes in *Asparagus officinalis*. *Sci. Rep.* 7: 41497.

Urich, M.A., Nery, J.R., Lister, R., Schmitz, R.J. and Ecker, J.R. (2015) MethylC-seq library preparation for base-resolution whole-genome bisulfite sequencing. *Nat. Protoc.* 10: 475–483.

Yakushiji, H. and Nakatsuka, A. (2007) Recent persimmon research in Japan. *Jpn. J. Plant Sci.* 1: 42–62.

Yang, H., Akagi, T., Kawakatsu, T. and Tao, R. (2019) Gene networks orchestrated by *MeGI*: a single-factor mechanism underlying sex determination in persimmon. *Plant J.* 98: 97–111.